POLITECNICO DI TORINO
Repository ISTITUZIONALE

Analysis of a protected Loss Of Flow Accident (LOFA) in the ITER TF coil cooling circuit

(Article begins on next page)

16 April 2024

Analysis of a protected Loss Of Flow Accident (LOFA) in the ITER TF coil cooling circuit

L. Savoldi, *Member, IEEE*, R. Bonifetto, N. Pedroni and R. Zanino, *Senior Member, IEEE*

Abstract— In moving towards ITER operation, the detailed analysis of fault conditions for the magnets becomes of increasing importance, to verify that the magnet protection system can safely manage them without any damage to the magnets. A "protected" Loss of Flow Accident in the ITER Toroidal Field (TF) coils, detected by the coil flow meters and managed by the Central Interlock System, is investigated here using the validated thermal-hydraulic code 4C. We simulate the entire sequence of events that is foreseen to protect the magnet, aiming at verifying the impact on the magnet. The LOFA consequences are investigated in terms of both the temperature margin in the winding pack and of the needed re-cooling time, which will affect the availability of the machine. It turns out that, for an "accelerated" discharge (i.e., a linear ramp-down) of the magnet current lasting less than 30 min, no quench should occur, while the corresponding re-cooling time should not exceed 1h. During the transient, ~ 10% of the He mass in the coil is vented to the quench tank due to the opening of the safety valves, and requires re-cooling.

Index Terms— ITER, superconducting magnets, LOFA, coil protection strategy, thermal-hydraulic simulation

I. INTRODUCTION

AS the manufacturing of the ITER superconducting magnets is proceeding [1]-[3], and after the systematic analyses of their normal operation, see e.g. [4]-[6], an effort towards the systematic investigation of the (dynamic) response of the magnet system under a wider range of *accidental* conditions is needed, aimed at guaranteeing its protection and integrity [7] in all possible fault scenarios.

An integrated approach to such an investigation will require several steps [8]-[10]:

(i) the identification by sensitivity analysis of the most important parameters (e.g., measured temperatures, pressures, …) and components (e.g., circulators, valves, controllers, …), that characterize and determine the behavior of the system [11];

(ii) the generation (by *possibly integrated* deterministic and probabilistic techniques) of a sufficiently large set of scenarios, representing the evolution of the system under several (off-normal) operating conditions (including different heat loads) [12], [13];

L. Savoldi, R. Bonifetto, N. Pedroni and R. Zanino are with the NEMO Group, Dipartimento Energia, Politecnico di Torino, 10129 Torino, Italy (e-mail: laura.savoldi@polito.it; roberto.bonifetto@polito.it; nicola.pedroni@polito.it; roberto.zanino@polito.it).

(iii) the identification of those (input) configurations that are capable of leading the system into a fault state. Such a "mapping" is of paramount importance, because in principle it allows to characterize and classify (in a timely manner, i.e. in a real-time control) a new developing scenario as 'safe' or 'faulty' [14].

Within this broad framework, we focus here on step (ii) and try to demonstrate the capability of the repeatedly validated 4C code [15]-[18], to perform *deterministic* analyses of accidental sequences: in particular, we concentrate on a detected Loss Of Flow Accident (LOFA), in both the winding pack (WP) and the casing cryogenic cooling circuits of an ITER Toroidal Field (TF) coil. (Note that, with reference to the specific problem at hand, the identification step (i) was implicitly carried out on the basis of engineering expertise and judgement, i.e., without the aid of specific sensitivity analysis techniques.)

While an undetected LOFA will result in a quench of the magnet [19], in the case of a detected LOFA, triggered by, e.g., the trip of the cold circulator, the protection strategy foresees first an "accelerated discharge" (AD) of the coil, followed by a controlled discharge of the Central Solenoid (CS) and of the Poloidal Field (PF) coils, while the plasma pulse is terminated and operation is stopped until the nominal operating conditions of the magnets are recovered [7].

Here we apply the 4C code to simulate the dynamics of detected total (cooling He mass flow rate reduction down to zero) and partial (mass flow rate reduction to an intermediate value between the nominal one and zero) LOFAs in an ITER TF cooling circuit, following the sequence of events on which the design of the coil protection system was based. The suitability of the protection strategy to bring the magnet to a "safe" state is evaluated assessing the temperature margin erosion in the WP during the AD, in order to confirm that no quench is initiated. The re-cooling time, needed to recover to normal operation conditions, is also assessed, together with the helium mass, if any, vented to the quench tank, in order to quantify both the additional thermal load on the refrigerator and the impact of a protected LOFA on the machine availability.

II. LOSS-OF-FLOW ACCIDENTAL SEQUENCE

A LOFA in the cooling circuit(s) providing the supercritical He (SHe) for the magnets cooling can be triggered by several initiating events [7]. Some of them are reported in Fig. 1 and namely: the power supply failure in the Auxiliary Cold Boxes
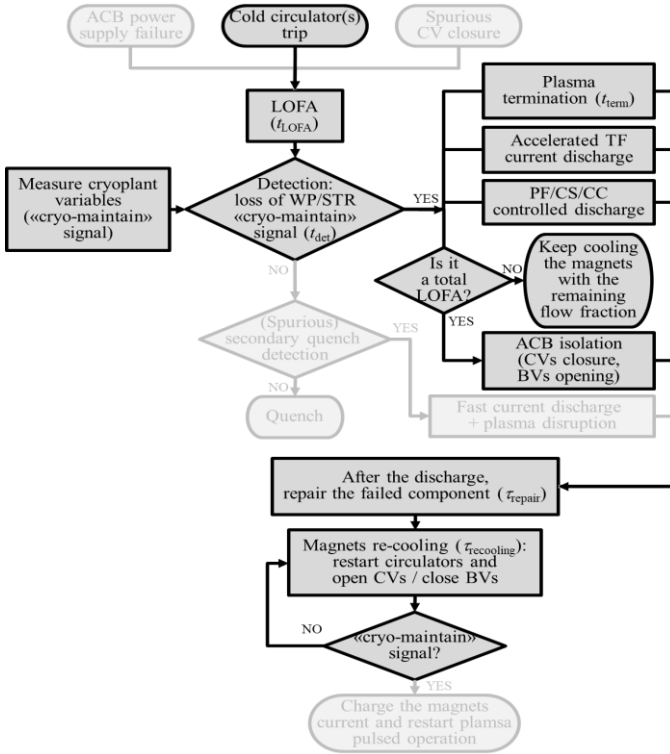
Fig. 1. Flow diagram of the accidental sequences involving a LOFA in the ITER TF magnet system cooling circuits [7]. The darkest sequence is analyzed in this paper.

(ACBs), the trip of the SHe cold circulator(s), the spurious closure of the Control Valves (CVs) controlling the SHe flow in the loops.

The flow diagram in Fig. 1 shows a first sequence of the events and main actions that can be taken by the Central Interlock System (CIS) according to [7], after the LOFA initiation, as described in detail in this Section and according to the timeline reported in Fig. 2. Note that the actual design of the actions to be taken in the operation of the ITER cryoplant in fault conditions will not necessarily be the same as presented in this paper, where some of the fault and recovery scenarios have been rather developed for demonstrative purposes. In Fig. 2a we see that the simulated LOFA is conservatively triggered after the End of Burn (EoB), see also below, while Fig. 2b reports the different times at which the actions listed in Fig. 1 are taken.
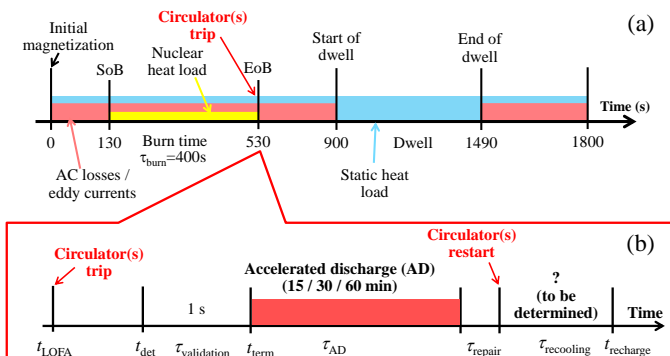

Fig. 2. Timeline (a) of the standard 15 MA plasma scenario (SoB = Start of Burn, EoB = End of Burn) and (b) of the events following a LOFA [7] in an ITER TF coil.

After the LOFA initiation, the accident may or may not be detected. In the latter case, no abnormal operation is detected in the cryoplant and the signal that the cryogenic operation is safe ("cryo-maintain" signal) is sent to the CIS. However, the mass flow rate reduction to nearly zero *at the coil inlet* may trigger a spurious secondary quench detection signal [20], inducing the Fast Discharge (FD) of the TF. If also the secondary quench detection fails, no other actions are taken and the transient (namely, the prosecution of the plasma scenario with nuclear heat deposition but without active cooling of the magnets) will lead to a quench of the TF coil [19].

On the other hand, the LOFA can be detected (at t_{det} in Fig. 2b) by the CIS measuring *relevant cryoplant variables* (discriminating the LOFA from a quench to avoid the triggering of a spurious FD): when they overcome selected thresholds, the "cryo-maintain" signal in the CIS is lost, thus triggering some actions in order to protect the magnets (and the cryoplant itself). In particular, in the case of loss of "cryo-maintain" signal in the cooling circuits (either the "WP loop" cooling the WP, or the "STR loop" cooling the structures (STR), or both), the following actions are taken [7], see Fig. 2b:

- plasma termination (at $t = t_{term}$) driven by the plasma control system;
- AD of the TF coils, i.e. the linear current ramp down from its nominal value (68 kA) to 0 kA in a given time (τ_{AD} = 30 min, nominally [7]);
- controlled discharge of PF, CS (and correction coils, if the LOFA is detected in the STR cooling circuit);
- inhibition of subsequent plasma pulses until the nominal operating conditions of all magnets are recovered.

As far as the cryoplant operation is concerned, a simplified sketch of the TF magnet cooling loops is reported in Fig. 3. The Auxiliary Cold Boxes (ACB) are highlighted, connected through the cryolines to the WP and STR by means of Control Valves (CVs) located in the Coil Termination Boxes (CTB) and Cold Valve Boxes (CVB) for the WP and STR loops, respectively. The ACBs mainly contain the circulators and heat exchangers, while the CTBs and CVBs contain the safety valves (SV), which open in case of pressure above 18 bar [21].

We distinguish between a total LOFA (when the measured variables indicate that the ~ 100% of the flow in the SHe loop is lost) and a partial LOFA, with only a reduction of the coolant flow. In the case of a total LOFA, the ACBs containing the liquid He (LHe) bath with the cold circulator and the heat exchangers (HXs), see Fig. 3, should be protected from possible overpressure (due to the pressurization in the WP or STR). The CVs will then be closed, and by-pass valves (BVs) opened to avoid a pressurization downstream the circulator, if the CVs are closed when it is not (yet) fully stopped (the BVs of the SHe pump in fact is supposed to open for pressure equilibrium between the suction and the discharge, in order to protect the pump itself as fail-safe condition).

When the coil discharge is completed and the whole energy stored in the magnets has been removed from the system, it is possible to intervene on the cold circulators to repair/restore them. After a given repair time (τ_{repair} in Fig. 2b), the circula-

TABLE I
SUMMARY OF THE TRIGGERING EVENTS AND ACTIONS TAKEN DURING THE MODELED LOFA [7].

Trigger	Time	Action	
		Total LOFA	Partial LOFA
Cold circulator(s) trip	t_{LOFA}	Simulated circulator speed exponential decrease to 0% ($\tau = \tau_{LOFA}$)	Simulated circulator speed exponential decrease to 50% ($\tau = \tau_{LOFA}$)
dm/dt_{in} and $dm/dt_{out} < dm/dt_{nom}/3$	$t_{det,part}$	-	Partial LOFA detection
$t_{det,part} + \tau_{validation}$	$t_{term,part}$	-	AD start
dm/dt_{in} and $dm/dt_{out} < dm/dt_{nom}/10$	t_{det}	Total LOFA detection	
$t_{det} + \tau_{validation}$	t_{term}	AD start, CVs closing[a], BVs opening[a]	CVs closing[a], BVs opening[a]
p at SV inlet > 18 bar	-	SV opening[b]	
Current AD end	$t_{term} + \tau_{AD}$	Stop power deposition due to AC losses	
Repair finished	$t_{term} + \tau_{AD} + \tau_{repair}$	Restart cold circulators	
$T_{op} \leq T_{initial}$	$t_{recharge}$	Start TF recharge[c]	

[a] In the loop where the dm/dt threshold is overcome.
[b] In the SV where the p threshold is overcome.
[c] Not simulated here.

tors can be restarted in order to perform the re-cooling of the magnet system after the LOFA. When the cryogenic operating conditions are recovered and the "cryo-maintain" signal restored in the CIS, the TF magnet system is re-charged and the plasma operation can be restarted.

III. SIMULATION OF A LOFA

A. 4C model of an ITER TF magnet

The 4C model of an ITER TF magnet was already described in detail in [4] and adopted for the simulation of a FD in [21]. It includes:

- the 7 double-pancakes wound with Nb3Sn cable-in-conduit conductors (CICCs);
- the structures, including the radial plates (RPs) and the casing;
- the two cryogenic cooling circuits supplying supercritical He (SHe) to the WP and to the casing cooling channels.

The cooling circuit model is also the same as in [21], with the addition of two Refill Valves (RVs), which have the purpose of refilling the two cooling loops during the re-cooling, as part of the SHe inventory could be vented to the quench tank through the opening of the SVs when the loop pressure overcomes the 18 bar threshold.

A single TF coil is simulated, as already done in [4], [21], relying on the fact that all TF coils are identical and series-connected from the electrical point of view, so their behavior should be the same during the AD. The circuit components (manifolds, pipelines, circulators) are properly rescaled to a single TF magnet, as done in [21].

B. Model of the LOFA sequence

All phases of the LOFA analyzed here are reported in Table I and described below.

The cold circulator trip triggering a LOFA is modeled as an exponential decrease (with time constant $\tau = \tau_{LOFA}$, assumed here to be = 1 s and parametrically varied up to 10 s) of the circulators rotational speed, down to 0 ("total" LOFA) or to 50% of the nominal value ("partial" LOFA).

The LOFA is triggered sufficiently close to (~ 5 s before) the End-Of-Burn (EoB, see Fig. 2a), in order to detect it and
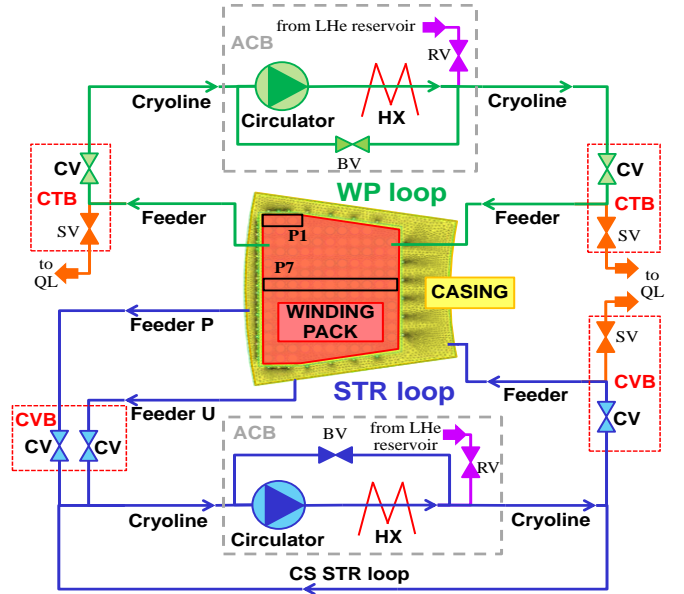

Fig. 3. Simplified scheme of the cryogenic cooling circuits of an ITER TF magnet. QL = Quench Line. The "P" and "U" feeders in the STR loop collect the He from the casing side facing the plasma and from all the other casing cooling channels, respectively (see the text for the definition of the other acronyms). The location of pancakes P1 and P7 in the WP is also highlighted.

start the AD very close to the EoB. This is a conservative approach, as at EoB the strands temperature reaches its maximum (and the temperature margin correspondingly its minimum ΔT_{marg}^{min}) due to the 400 s nuclear heat deposition foreseen in the 15 MA plasma scenario: the AC losses during the AD will then deposit additional power in the TF when they are at their warmest temperature in the whole cycle.

The LOFA detection (at $t = t_{det}$ in Fig. 2b) is assumed here to rely only on the *dm/dt* measurements at the inlet and outlet of the WP and of the casing. A total LOFA in either of the loops is then detected when the *dm/dt* at both inlet and outlet of the magnet cooling paths of that loop is simultaneously smaller than a detection threshold, defined as $(dm/dt)_{nom} / k$, where $(dm/dt)_{nom}$ is the nominal *dm/dt* of that loop. In the case of a total LOFA, we assume $k = 10$. The simultaneous verification of the above-mentioned condition at inlet and outlet should help in discriminating a LOFA (when both *dm/dt* are supposed to reduce) from a secondary quench detection signal (when only the inlet *dm/dt* is supposed to reduce, due to the He pressurization in the quenched CICC, while the outlet *dm/dt* will increase).

The LOFA detection is validated (to avoid spurious detections due to possible high frequency *dm/dt* measurements oscillations or spikes) waiting for a time $\tau_{validation} = 1$ s, throughout which the *dm/dt* at the magnet boundaries remains below the detection threshold, before triggering the plasma termination at $t_{term} = t_{det} + \tau_{validation}$. We assume here that the plasma termination does not impact, in terms of additional heating, on the TF coil. Simultaneously, the AD starts, the CVs close and the BV opens in the ACB of the loop where the LOFA is detected, so that the potentially still operating cold circulator of the other loop can cool the magnet also during the AD. The valves closure (or opening) lasts 1 s in the simulation.

In the case of a partial LOFA, we set $k = 3$ in the detection threshold. As the cooling capability of the SHe loop in that case is not fully lost but only strongly reduced, the ACBs are not isolated. The CVs are then left open, so that the remaining SHe flow rate can provide a partial cooling of the magnet during the AD. In the case of a further *dm/dt* reduction below 10% of the nominal value during the transient, the ACB will be protected closing the CVs.

The AD duration (τ_{AD} in Fig. 2b) in the simulations is varied parametrically from 15 min to 60 min, i.e. ½ and twice the nominal one [7] of 30 min, respectively. The TF current (and correspondingly also the magnetic field) is ramped down linearly from its nominal value (68 kA) to 0 kA, thus inducing a significant heat deposition in the bulky stainless-steel (SS) structures (including here casing + RPs) and in the conductors, due to AC losses (eddy currents and coupling losses, respectively). The associated power deposition, for the three τ_{AD} values considered here, has been estimated from that computed during a current FD [21], under the reasonable assumption that the magnetic field acting on the TF coil is mostly self-field and that the power deposited in both structures and conductors is directly proportional to the square of the magnetic field variation. The eddy currents in the bulky SS structures are responsible of a power generation more than 3 orders of magni-

tude larger than that induced by AC losses in the conductors (~ 0.8 W and 2.5 kW, respectively, in the case $\tau_{AD} = 30$ min).

At the end of the AD, when the power deposition is also back to zero, a τ_{repair} of 150 s has been assumed for computational time convenience. In reality, this duration could be much longer, e.g. if an ACB warm-up is required to manually change the cold circulator.

The magnets re-cooling is then simulated, assuming it is directly performed by the He loop (no direct connection with the refrigerator to cooldown and pressurize to the nominal operating condition), aiming at comparatively assess the $\tau_{recooling}$ duration after the different τ_{AD}. The simulation is stopped when the initial nominal cryogenic conditions (namely, mass flow rate, temperature and pressure in the cooling circuits) are restored in the TF magnet.

IV. RESULTS

We consider here three different cases for a total LOFA: the case in which it occurs simultaneously in the WP and STR loops, as well as the two cases when it occurs only in one of the two circuits, to assess the different impacts in terms of coil temperature margin and hot spot. The case of a partial LOFA occurring simultaneously in both loops is also analyzed.

A. Total LOFA in the WP and STR circuits

The evolution of the mass flow rate (*dm/dt*) computed in the WP in the first seconds after the LOFA and throughout the entire transient up to the end of the magnet re-cooling is reported in Fig. 4a and Fig. 5a, respectively. In the former, the evolution of *dm/dt* at the circulator is shown to be much sharper than that at the inlet and outlet of the WP. This is due to the characteristic of the circulator (which enters in the surge region, see below), while the difference in the computed WP inlet and outlet values is due to the compressibility of the SHe. In the case when the reduction of the flow occurs on the ~ 1 s time-scale (τ_{LOFA}), the signal measured at the circulator would then be the most suitable for the detection of the LOFA in view of the rapid decrease below the threshold value.

In the present analysis, however, the LOFA detection relies conservatively on the WP flow meters, see above, and the LOFA detection in the WP cooling loop occurs ~ 6 s after the circulator trip. The WP inlet and outlet pressure converge to an intermediate value before the opening of the CVs, due to the drop of the *dm/dt*, see Fig. 4b. At the time when the AD starts (~ 7.5 s after the trip of the circulator) the mass flow rate in the WP is already close to zero, but it further decreases becoming negative both at the WP inlet and outlet due to the simultaneous start of the power deposition, in turn caused by the current decrease, and the full closing of the CVs (as reported in Fig. 4c), which induces a quick pressure rise of the downstream manifold, see Fig. 4b.

The evolution of *dm/dt* and pressure in the WP during the rest of the transient, reported in Fig. 5a and b, reveals that the *dm/dt* reacts at the opening of the SVs (at $t - t_{LOFA} \sim 950$ s in Fig. 5c), which is induced by the pressure rise to the threshold
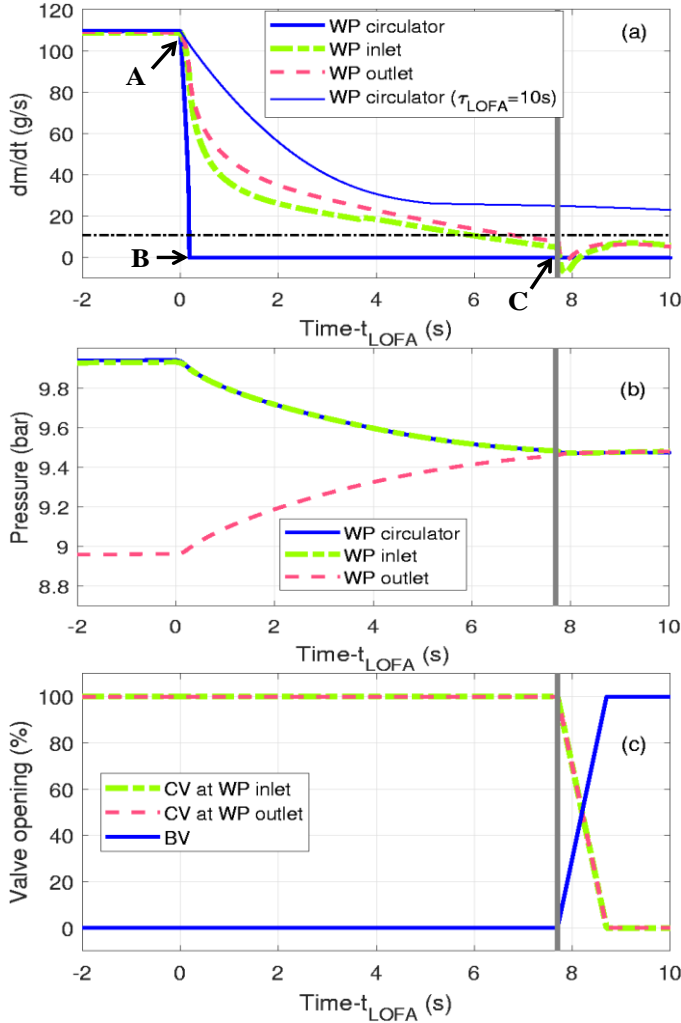
Fig. 4. Simulation of the first phases of a total LOFA ($\tau_{LOFA} = 1$ s) in both cooling loops of a TF coil with $\tau_{AD} = 30$ min. (a) Computed evolution of WP mass flow rate at circulator (including also the case with $\tau_{LOFA} = 10$ s, see the text), coil inlet and coil outlet; the detection threshold, set to 10% of the nominal mass flow rate, is also reported (dash-dotted black horizontal line) in order to allow the identification of the WP circuit CVs opening time, 1 s after the detection (vertical solid line). (b) Computed evolution of the He pressure at circulator, coil inlet and coil outlet. (c) CVs and BV opening fractions.
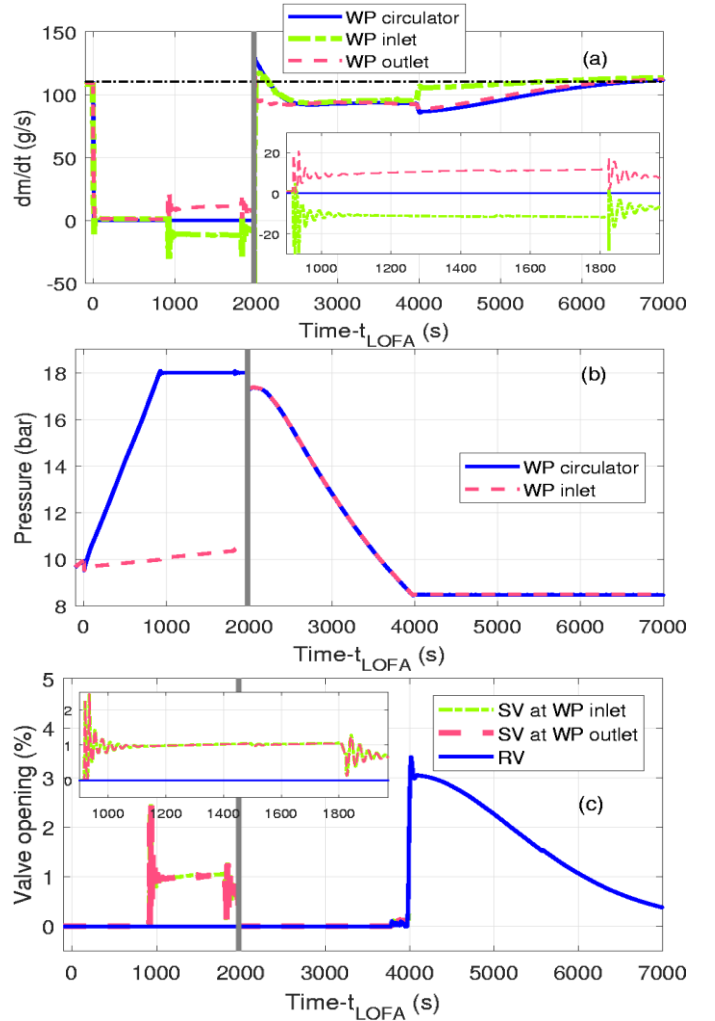

Fig. 5. Simulation of a total LOFA in both cooling loops of a TF coil with $\tau_{AD} = 30$ min. Computed evolution of (a) WP mass flow rate at circulator, coil inlet and outlet, (b) pressure at WP circulator outlet and coil inlet during the whole LOFA, and (c) SVs and RV opening fraction; the circulators restart time is marked as a vertical solid line, while in (a) the horizontal dash-dotted black line is the initial mass flow rate value. In (a) and (c) the zoom on the phase during which He is vented through the SVs is reported in the inset.

of 18 bar, see Fig. 5b, and to the end of the AD (at ~ 1800 s since $\tau_{AD} = 30$ min, see Fig. 5a). In between the two above-mentioned times, the helium is vented out of the WP, as revealed by the negative dm/dt value at the WP inlet and positive at the WP outlet, and as reported in Fig. 5c, showing the WP circuit SVs (and RV) opening.

At the time the circulator is restarted and the CVs closed, the dm/dt quickly goes back to a steady value which is slightly lower than the initial one (see Fig. 5a) – in fact it cannot go back to the initial operating values since some mass (~ 27 kg of gaseous He) has been vented through the SVs to the quench tank. The pressure during the re-cooling phase reaches the initial operating value but it would further decrease, if the RV didn't open. The action of the RV allows the refilling of the vented helium in the loop and forces the pressure to stabilize at the initial operating condition ($t - t_{LOFA} \sim 4000$ s in Fig. 5b

and c). The total re-cooling time is ~ 1 h, after which the TF operating conditions are restored.

The trajectory of the WP cold circulator operating point during the total LOFA (Fig. 6a) shows that the reduction of the speed of the circulator, in the case of $\tau_{LOFA} = 1$ s, causes a decrease of the circulator dm/dt at ~ constant pressure head Δp (~ horizontal A-B segment in Fig. 6a, see also Fig. 4a), since reverse flow in the circulator is not allowed and the high hydraulic impedance of the WP does not allow the pressure at its inlet and outlet to quickly equalize. Although this brings the circulator into the surge zone (shaded area in Fig. 6a), the unsteady behavior resulting from the crossing of the surge line is damped by the circulator trip. The collapse of the pressure head (vertical B-C segment in Fig. 6a, see also Fig. 4a) follows. The restart of the circulator and restore of the operating conditions allow closing the trajectory loop. The restart trajectory is different from the trip one in view of the different thermodynamic conditions during the two transients. Note that
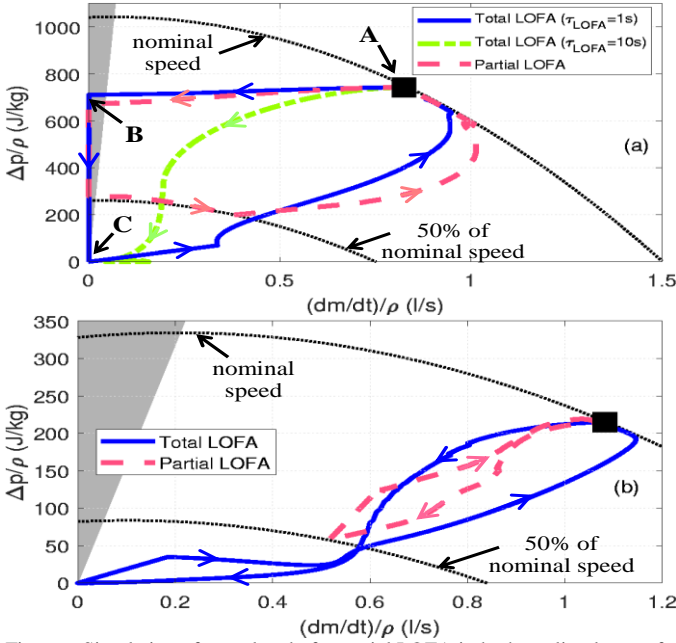
Fig. 6. Simulation of a total and of a partial LOFA in both cooling loops of a TF coil with $\tau_{AD} = 30$ min. Characteristic curves [22] at nominal speed and at 50% of nominal speed and computed trajectories of: (a) the WP loop cold circulator, and (b) the STR loop cold circulator. The nominal operating point is also reported (solid square), as well as the region behind the surge line (shaded area).

a longer τ_{LOFA} (e.g. ≥ 10 s) will instead allow the operating point during the accident to stay far from the surge region, as shown also in Fig. 6a, as both the circulator dm/dt and the pressure drop will decrease on a similar time-scale.

The dm/dt and pressure qualitative evolution are independent of the duration of the current discharge.

As far as the STR cooling loop is concerned, the evolution of the mass flow rate in the first seconds after the LOFA is reported in Fig. 7. Note that here the difference between the dm/dt value computed at different locations in the loop is almost negligible: being the total He volume in the STR loop much smaller ($\sim 1/5$) than in the WP loop, the inertia and compressibility effects are also smaller, so that any location would be $\sim$ equivalent to detect the LOFA in this circuit. The detection time here is ~ 2.5 s from the circulator trip, and after ~ 3.5 s the ACB is disconnected from the STR, closing the CVs, see Fig. 7c. From that time on, the pressure at the circulator remains constant (Fig. 7b), while that in the STR keeps increasing due to the fact that the power deposition in the structures is orders of magnitude higher than in the conductors (and the He volume in the STR loop is much smaller than in the WP one).

The computed trajectory of the STR circulator in its characteristic space is reported in Fig. 6b, highlighting a different behavior with respect to the trajectory followed by the WP cold circulator. In fact, the shorter cooling paths allow a faster pressure redistribution in the STR circuit, on the same time-scale of the circulator mass flow rate decrease, so that the circulator trajectory does not go beyond the surge line during the LOFA: the mass flow rate reduction is then much smoother than in the WP circulator case, even for a $\tau_{LOFA} = 1$ s.
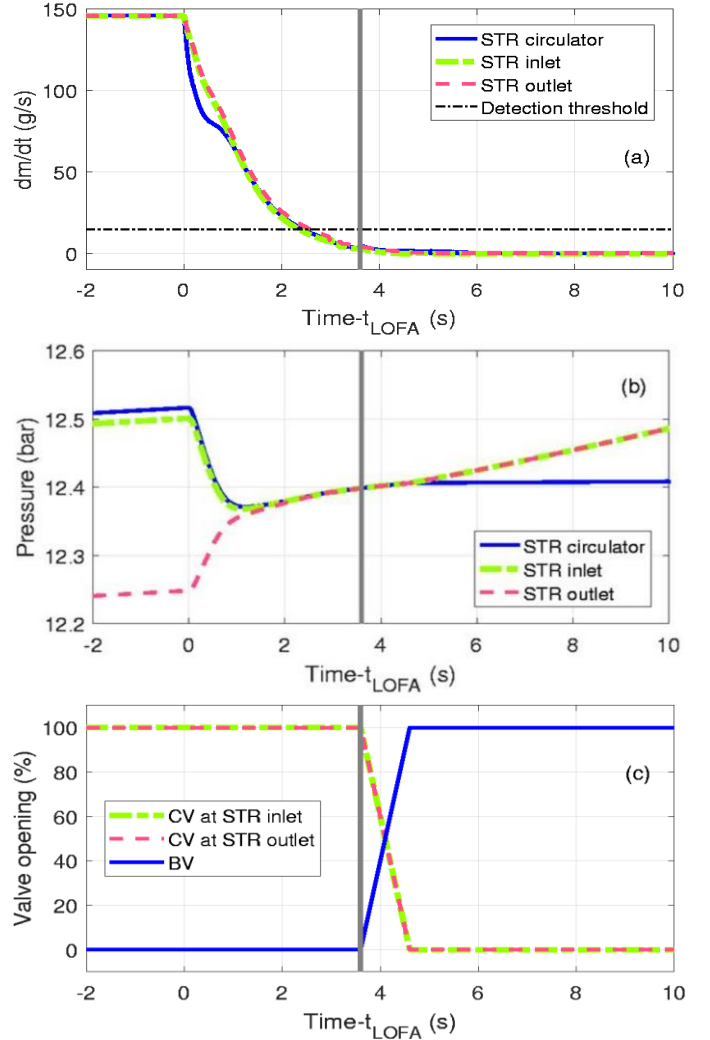

Fig. 7. Simulation of the first phases of a total LOFA in both cooling loops of a TF coil with $\tau_{AD} = 30$ min. Computed evolution of (a) mass flow rate and (b) pressure at the STR circulator, coil inlet and coil outlet during the first phases of a LOFA; the LOFA detection threshold, set to 10% of the nominal mass flow rate, is also reported (dash-dotted horizontal line) in (a), in order to allow the identification of the STR circuit CVs opening time, 1 s after the detection (vertical solid line). (c) CVs and BV opening fractions.

To allow a proper evaluation of the re-cooling time, the evolution of the maximum temperature in the structures (T_{max}^{STR}) during the AD following the LOFA is reported in Fig. 8 for the two shortest τ_{AD} (15 min and 30 min, respectively), for which we expect the highest values of T_{max}^{STR}. The peak value is ~ 22 K in the worst case – since the initial hot spot in the STR is ~ 14 K, the temperature increase due to the AC losses induced by the AD is very limited, but no possible effect of the forced plasma shut-down are taken into account in the simulation. The re-cooling time ($\tau_{recooling}$) needed to recover the initial condition is slightly longer in the case of $\tau_{AD} = 15$ min, with respect to the case $\tau_{AD} = 30$ min, as expected since higher temperatures are reached, but in this specific case (repair time τ_{repair} almost negligible), the unavailability (defined as $\tau_{AD} + \tau_{repair} + \tau_{recooling}$) of the TF coil turns out to be comparable (~ 2 h) independently on the value of τ_{AD}. Note that in Fig. 8 the T_{max}^{STR} after the re-cooling is smaller than the initial value because the latter refers to the beginning of a *pe-*
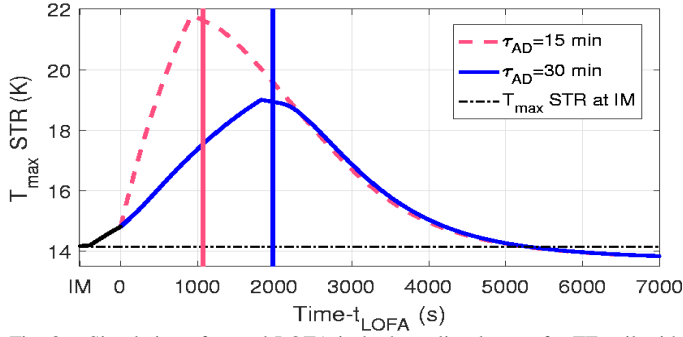
Fig. 8. Simulation of a total LOFA in both cooling loops of a TF coil with $\tau_{AD} = 15$ min and 30 min. Computed evolution of T_{max}^{STR}. The circulators restart time is marked as a vertical line. The initial maximum temperature in the STR (at initial magnetization, IM, of the periodic pulse) is also reported (dash-dotted horizontal line) in order to identify the re-cooling time.

Fig. 9. Simulations of a total LOFA in both cooling loops of a TF coil with different τ_{AD}. Computed evolution of the ΔT_{marg}^{min} on pancakes P1 (a) and P7 (b) during the total LOFA in a TF coil. The circulators restart time is marked as a vertical line, while the solid star indicates the time at which the quench is triggered during the 60 min AD.

riodic plasma pulse. A He mass of ~ 27 kg (~ 10% of the total inventory in a TF magnet circuit) is vented to the quench tanks in the $\tau_{AD} = 30$ min case (~ 54 kg if $\tau_{AD} = 15$ min). This mass has to be brought back to cryogenics temperature.

The suitability of the magnet protection strategy adopted in the case of a LOFA is then assessed evaluating the effects of the AC losses during the AD on the minimum temperature margin ΔT_{marg}^{min} in the WP, to check if the margin remains positive or if it becomes negative triggering a quench, and considering different possible durations of the current discharge. In fact, from one side the heat source will be lower for longer τ_{AD} because of the smaller current (and magnetic field) variation, but at the same time the current sharing temperature (T_{CS}) will increase slower if the current discharge occurs on a longer τ_{AD}, so that it is not trivial to understand which effect between the two will drive the transient evolution.

In Fig. 9 the evolution of ΔT_{marg}^{min} is reported for the lateral and central pancakes in the WP (P1 and P7, respectively), which are the two most critical locations from the point of view of the ΔT_{marg}^{min} [5]. The slope changes are due to the spatial change of the ΔT_{marg}^{min} location along the pancake length.

The simulations show that no risk of quench is present with $\tau_{AD} \leq 30$ min, while a quench is initiated in the lateral pancake few mins after the beginning of the AD for the longest τ_{AD} tested here. The magnet protection strategy from [7] seems thus adequate in case of a total LOFA, provided the AD duration does not exceed 30 min.

The quench is initiated at the outlet joint of P1, conservatively considered adiabatic with respect to the bus bar (also involved in the LOFA). Thus the joint represents the weakest point of the magnet stability during a LOFA due to the fact that in that short conductor (just 3 turns, to be compared to the 11 turns of the central pancakes) the value of the magnetic field at the joint location is ~ 6 T at full current (~ 1 T for the central pancakes) and the current sharing temperature T_{CS} is still as low as ~ 10 K after ~ 300 s – at the same time, the conductor temperature at the joint has increased form the initial value of 5.5 K to 10 K in view of the joule power generation (due to a total joint resistance of 2 nΩ [6]), resulting in a quench, see Fig. 10. Note, however, that while the analysis of the quench development and propagation is beyond the scope

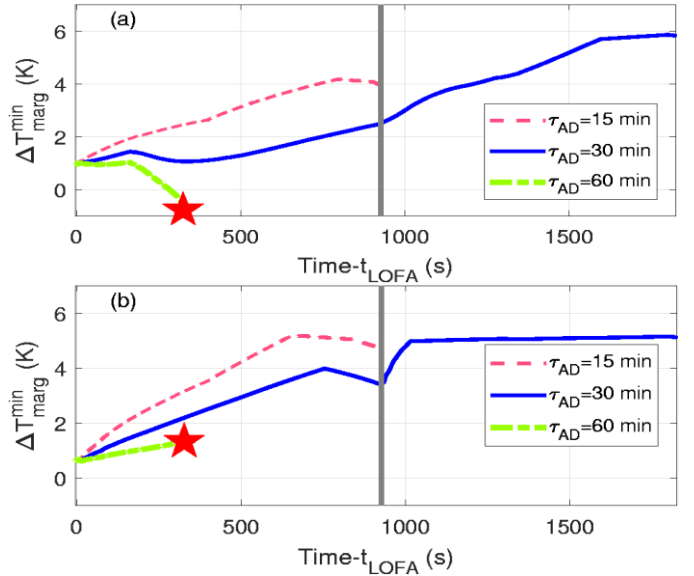of the present study, it would be worthwhile to check if, from the one hand, it is detectable with the protection system currently foreseen (low voltage level) and, from the other hand, if the possible trigger of a FD could be of any danger for the system.

B. Total LOFA in WP or STR circuit only

The effect of a total LOFA occurring either in the WP or in the STR loop only has been also analyzed, with $\tau_{AD} = 30$ min, and the results are reported in Fig. 11 in terms of effects on the ΔT_{marg}^{min} for the WP loop and on T_{max}^{STR} for the STR loop, respectively. It is shown that the LOFA in only one of the two loops always leads to similar or lighter effects. In particular, in terms of reduction of the temperature margin a LOFA in the WP circuit only has consequences very similar to the LOFA in both circuits, see Fig. 11a. Similarly, when considering the increase of the hot spot temperature in the structures, see Fig. 11a, a LOFA in the STR circuit only will lead to consequences similar to a LOFA in both loops, while the temperature margin
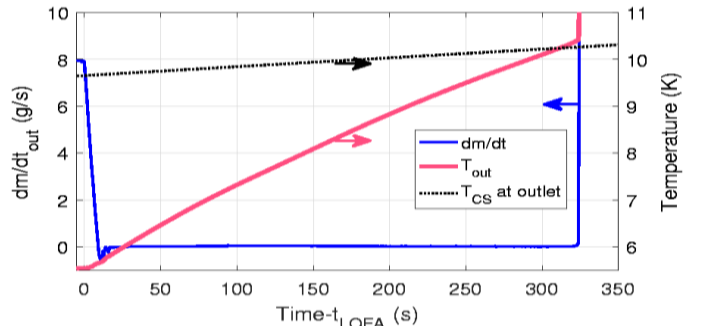

Fig. 10. Simulation of a total LOFA in both cooling loops of a TF coil with $\tau_{AD} = 60$ min. Computed evolution of the strand temperature and T_{CS} at the outlet of the P1 joint (right y-axis) and of the P1 outlet mass flow rate (left y-axis). A quench is initiated at ~ 325 s (see the sudden T_{out} and dm/dt_{out} increase at that time).
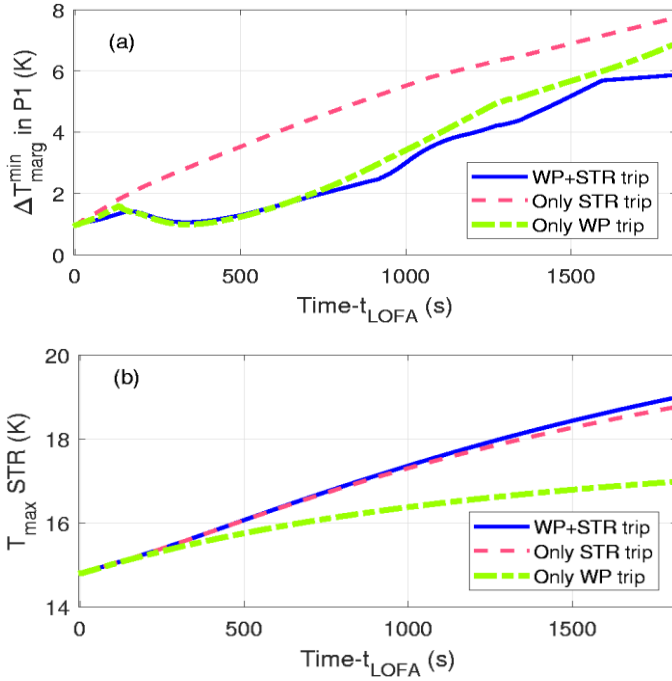
Fig. 11. Simulation of a total LOFA with $\tau_{AD} = 30$ min. Comparison between the computed evolution of (a) ΔT_{marg}^{min} in P1 and (b) T_{max}^{STR} in case of the circulator trip in both WP and STR cooling circuit, in the STR cooling circuit only and in the WP cooling circuit only.

Fig. 12. Simulation of the first phase of a partial LOFA in both cooling loops of a TF coil with $\tau_{AD} = 30$ min. Computed evolution of the WP (a) and STR (b) He mass flow rate at the cold circulator and at the coil inlet and outlet. In (a), the corresponding curves for $\tau_{LOFA} = 10$ s are also reported (thin curves).

will not be of any concern during this transient.

C. Partial LOFA in WP and STR circuits

The evolution of the mass flow rate in both circuits during the first phase of a partial LOFA is reported in Fig. 12. The detection threshold set to 30% of the nominal mass flow rate in each loop (see Table I) is overcome only in the WP circuit (Fig. 12a), where the cold circulator operating point is driven to the surge zone also in this case of 50% speed reduction, as shown in Fig. 6a. No LOFA detection is triggered in the STR loop (see Fig. 12b), and no CVs closure is driven in this case, so that ~ 50% of the SHe is still circulated in both cooling circuits also during the AD. As a result, the consequences of the LOFA are strongly mitigated with respect to a total LOFA, with the margin in pancakes P1 and P7 staying well above the corresponding evolution during a total LOFA (not shown).

Note however that if e.g. τ_{LOFA} is longer, the partial LOFA may be undetected, as shown in Fig. 12, especially if the detection is based only on the signal of the flow meters located at the coil inlet/outlet.

V. CONCLUSIONS AND PERSPECTIVE

As a first step towards a more systematic analysis of the dynamic response of the ITER superconducting magnets in accidental conditions, the deterministic analysis of a protected LOFA in the cooling loops of an ITER TF coil has been performed with the 4C code, considering parametrically the duration of the accelerated discharge of the coil, foreseen after the LOFA to protect the coil.
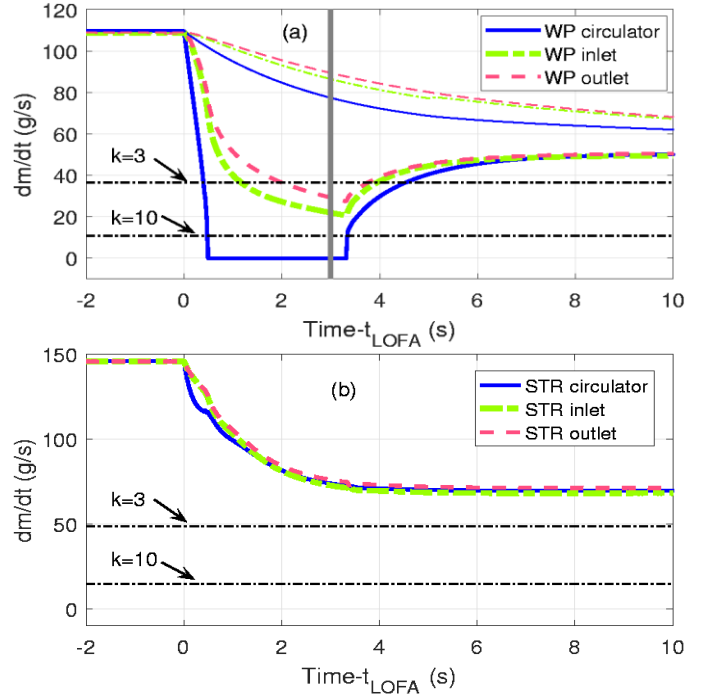
The detection of the LOFA should be based not only on the *dm/dt* measurements at the coil inlet and outlet, but also at the cold circulator(s), which will react faster to the LOFA (at least if it is initiated by a cold circulator trip).

If a total LOFA occurs simultaneously in both the WP and the STR circuits, a quench is initiated only in the case of a long (60 min) discharge time, in the joint region of the P1.

For all discharge times analyzed here, a strong He pressurization in the magnet, caused by the AC losses during the TF coil discharge in the absence of active cooling, causes the opening of the safety valves, with the venting of 10-20% of the total He inventory in the magnet to the quench tanks.

The computed re-cooling time after the LOFA is ~ 1 h, if the current discharge time is 30 min.

While a total LOFA in only one of the two cooling loops does not show criticalities, in case of a partial LOFA some attention should be devoted to the detection threshold and strategy, in order to reduce the probability to have undetected accidents.

In this respect, the purely deterministic approach pursued here could be efficiently complemented by a probabilistic analysis to perform a more complete and systematic assessment of the accident scenarios possibly developing in a complex, dynamic fusion system like ITER.

REFERENCES

[1] A. Bonito Oliva, E. Barbero Soto, R. Batista, B. Bellesia, E. Boter Robello, J. Buskop, J. Caballero, M. Casas Lino, M. Cornelis, J. Cornella, D. Kleiner, C. Kostopoulos, K. Libens, A. Moreno, L. Poncet, R. Harrison, A. Barutti, O. Dormicchi, C. D'Urzo, P. Pesenti, N. Valle,

A. Loizaga, J. Lucas, F. Pando, A. Felipe, R. Francone, M. Bolla, P. Barbero, J. Silva Ribeiro, D. Rossi, E. Theisen, and H. Scheller, "Progress in Europe of the Procurement of the EU ITER TF Coils," *IEEE Trans. Appl. Supercond.*, vol. 26, issue 4, Jun. 2016, Art. ID 4205106.

[2] T. Hemmi, K. Matsui, H. Kajitani, T. Sakurai, M. Yamane, T. Mizutani, K. Sakaguchi, M. Nakamoto, T. Nakano, K. Takano, S. Ando, M. Iguchi, E. Fujiwara, T. Saito, S. Hwang, N. Tanaka, T. Hanaoka, M. Nakahira, and N. Koizumi., "Development of ITER Toroidal Field Coil in Japan," *IEEE Trans. Appl. Supercond.*, vol. 27, issue 4, Jun. 2017, Art. ID 4200105.

[3] B. Bigot, and N. Mitchell, "Overall Status of the ITER Project," *this conference*.

[4] R. Bonifetto, F. Buonora, L. Savoldi Richard, and R. Zanino, "4C code simulation and benchmark of ITER TF magnet cool-down from 300 K to 80 K," *IEEE Trans. Appl. Supercond.*, vol. 22, issue 3, Jun. 2012, Art. ID 4902604.

[5] L. Savoldi Richard, R. Bonifetto, A. Foussat, N. Mitchell, K. Seo, and R. Zanino, "Mitigation of the Temperature Margin Reduction due to the Nuclear Radiation on the ITER TF Coils," *IEEE Trans. Appl. Supercond.*, vol. 23, issue 3, part 2, Jun. 2013, Art. ID 4201305.

[6] L. Savoldi Richard, R. Bonifetto, U. Bottero, A. Foussat, N. Mitchell, K. Seo, and R. Zanino, "Analysis of the effects of the nuclear heat load on the ITER TF magnets temperature margin," *IEEE Trans. Appl. Supercond.*, vol. 24, issue 3, Jun. 2014, Art. ID 4200104.

[7] Central Interlock System Strategy for ITER Magnet Protection: Machine Protection Functions, ITER_D_K7G8GN v2.1, January 24, 2014.

[8] T. Aldemir, "A survey of dynamic methodologies for probabilistic safety assessment of nuclear power plants," *Annals of Nuclear Energy*, vol. 52, 2013, pp. 113-124.

[9] E. Zio, "Integrated deterministic and probabilistic safety assessment: Concepts, challenges, research directions," *Nucl. Eng. Des.*, vol. 280, 2014, pp. 413-419.

[10] P. Turati, N. Pedroni, and E. Zio, "Simulation-based exploration of high-dimensional system models for identifying unexpected events," *Reliability Engineering and System Safety*, vol. 165, 2017, pp.317-330.

[11] E. Borgonovo, and E. Plischke, "Sensitivity analysis: A review of recent advances," *European Journal of Operational Research*, vol. 248, issue 3, 2016, pp. 869-887.

[12] K. H. Kernstine, "Inadequacies of Traditional Exploration Methods in Systems-of-Systems Simulations," *IEEE Systems Journal*, vol. 7, issue 4, 2013, pp. 528-536.

[13] F. Di Maio, A. Bandini, E. Zio, A. Alfonsi, and C. Rabiti. "An approach based on Support Vector Machines and a K-D Tree search algorithm for identification of the failure domain and safest operating conditions in nuclear systems," *Progress in Nuclear Energy*, vol. 88, 2016, pp. 297-309.

[14] D. Maljovec, S. Liu, B. Wang, D. Mandelli, P.T. Bremer, V. Pascucci, and C. Smith. "Analyzing simulation-based PRA data through traditional and topological clustering: A BWR station blackout case study," *Reliability Engineering & System Safety*, vol. 145, 2016, pp. 262-276.

[15] L. Savoldi Richard, F. Casella, B. Fiori, and R. Zanino, "The 4C code for the cryogenic circuit conductor and coil modeling in ITER," *Cryogenics*, vol. 50, no. 3, Mar. 2010, pp. 167-176.

[16] R. Zanino, R. Bonifetto, R. Heller, and L. Savoldi Richard, "Validation of the 4C Thermal-Hydraulic Code against 25 kA Safety Discharge in the ITER Toroidal Field Model Coil (TFMC)," *IEEE Trans. Appl. Supercond.*, vol. 21, no. 3, Jun. 2011, pp. 1948-1952.

[17] R. Zanino, R. Bonifetto, C. Hoa, and L. Savoldi Richard, "Verification of the Predictive Capabilities of the 4C Code Cryogenic Circuit Model," *AIP Conf. Proc.*, vol. 1573, 2014, pp. 1586-1593.

[18] R. Zanino, R. Bonifetto, A. Brighenti, T. Isono, H. Ozeki, and L. Savoldi, "Prediction, experimental results and analysis of the ITER TF Insert Coil quench propagation tests, using the 4C code," *presented at this conference and submitted to Supercond. Sci. Technol.* (2017).

[19] L. Savoldi, R. Bonifetto, and R. Zanino, "Analysis of a loss-of-flow accident (LOFA) in a tokamak superconducting Toroidal Field Coil," *Safety and Reliability – Theory and Applications*, 2017, pp. 67-74.

[20] S. Nicollet, D. Bessette, D. Ciazynski, M. Coatanéa-Gouachet, J. L. Duchateau, B. Lacroix, and F. Rodriguez-Mateos, "Thermal Behavior and Quench of the ITER TF System During a Fast Discharge and Possibility of a Secondary Quench Detection," *IEEE Trans. Appl. Supercond.*, vol. 22, no. 3, Jun. 2012, Art. ID 4704304.

[21] L. Savoldi Richard, D. Bessette, R. Bonifetto, and R. Zanino, "Parametric analysis of the ITER TF fast discharge using the 4C code," *IEEE Trans. Appl. Supercond.*, vol. 22, issue 3, Jun. 2012, Art. ID 4704104.

[22] H.-S. Chang, H. Vaghela, P. Patel, A. Rizzato, M. Cursan, D. Henry, A. Forgeas, D. Grillot, B. Sarkar, S. Muralidhara, J. Das, V. Shukla, and E. Adler, "Status of the ITER Cryodistribution," *Proceedings of CEC/ICMC* 2017.